JOURNAL OF MATERIALS SCIENCE 29 (1994) 1222–1226

Preparation of bimodal porous mullite ceramics

H. ABE, H. SEKI, A. FUKUNAGA
Ceramic Research Center of Nagasaki, 605-2 Hiekoba-go, Hasami-cho, Higashi-sonogi-gun, Nagasaki 859-37, Japan

M. EGASHIRA
Department of Materials Science and Engineering, Faculty of Engineering, Nagasaki University, 1-14 Bunkyo-machi, Nagasaki 852, Japan

Bimodal porous ceramics were prepared based on the needle-like mullite crystals, by leaching the glass matrix of the calcined body of the kaolin and transition metal oxide systems mixed with coal powder or polymethylmethacrylate beads as a pore-forming material. Small and large pores in the bimodal porous ceramics were in the range of 0.06–0.5 and 3–7 μm, respectively. The small pores originated from gaps between the needle-like crystals, while the large ones originated from the pore formers. However, the large pores were suggested to be ink-bottle type in shape, because the measured size was much smaller by approximately an order of magnitude than the diameter of the pore former. In every case, the total and large pore volumes agreed well with those calculated based on the density and composition of the starting materials and the intrinsic porosity of the mullite ceramics.

1. Introduction

Inorganic porous materials, typically active charcoal and zeolite, have high performance adsorption and catalytic properties [1–3], and are now widely used as adsorbents, deodorants, decolorizers, catalyst supports, and so on, in various chemical and food industries. These properties originate mainly from their large surface areas due to micropores in the materials. Such porous materials also contain a considerable amount of macropores. The macropores do not contribute to the surface characteristic properties mentioned above, but promote diffusion of a fluid into micropores.

On the other hand, utilization of various types of porous materials with relatively small surface areas has been increasing recently in many fields such as the food [4], fermentation [5, 6] industries, industrial waste-water treatment [7, 8], and medical care [9]. Typical examples are filters for solid and liquid separation, supports for biocatalysts such as enzymes and bacteria, and column packings of chromatography. In these materials, it is desired to have large pores as well, as in the cases of active charcoal and zeolite, to ensure better permeation or better contact between fluids and porous materials. Thus, it is very important to have the bimodal pore structure. A honeycomb structure is another typical example, although the size of the larger pores is extremely large.

We have developed porous ceramics consisting of needle-like mullite crystals [10, 11], by leaching the glass matrices of the calcined bodies of the kaolin–transition metal oxide systems with a sodium hydroxide or mixed acid solution. The median pore size could be controlled in the range 0.05–2.0 μm with relatively narrow pore distribution. In the present work, addition of coal powder and polymethylmethacrylate beads as a large pore-forming agent into the starting materials has been attempted to develop the bimodal pore structure. The usefulness of coal powder addition has been reported in the case of cordierite ceramics [12].

2. Experimental procedure

2.1. Preparation of mullite ceramics

New Zealand kaolin was used as the starting material of the porous mullite ceramics. Three kinds of transition metal oxides, titanium, iron and cobalt, were mixed all together with the kaoline. These transition metal oxides promote growth of needle-like mullite crystals [11]. The amount of each oxide was 3.0 wt %. This was designated sample A. In sample B, only cobalt oxide of 5 wt % was mixed with the kaolin, while in sample C only copper oxide of 5 wt % was used. The sample mixtures were suspended in distilled water containing sodium polyacrylate (Toa Gosei Co., T-40) of 1.2 wt %, the water content being 50 wt %, and the suspensions were completely mixed in a pott-mill for 16 h. Then coal powder (Australian Blair Athol coal, 50–100 μm) or polymethylmethacrylate beads (PMMA, Soken Chemical Co., MR60G, 60 μm) were added to the suspensions in amounts of 45 wt % on a dried basis. These additives act as a large pore-forming agent because they burn out during firing. The pore formers were well homogenized into the suspensions by magnetic stirring *in vacuo*. The samples obtained with pore formers were designated, for example, samples AC and BP, the latter letters C and

0022–2461

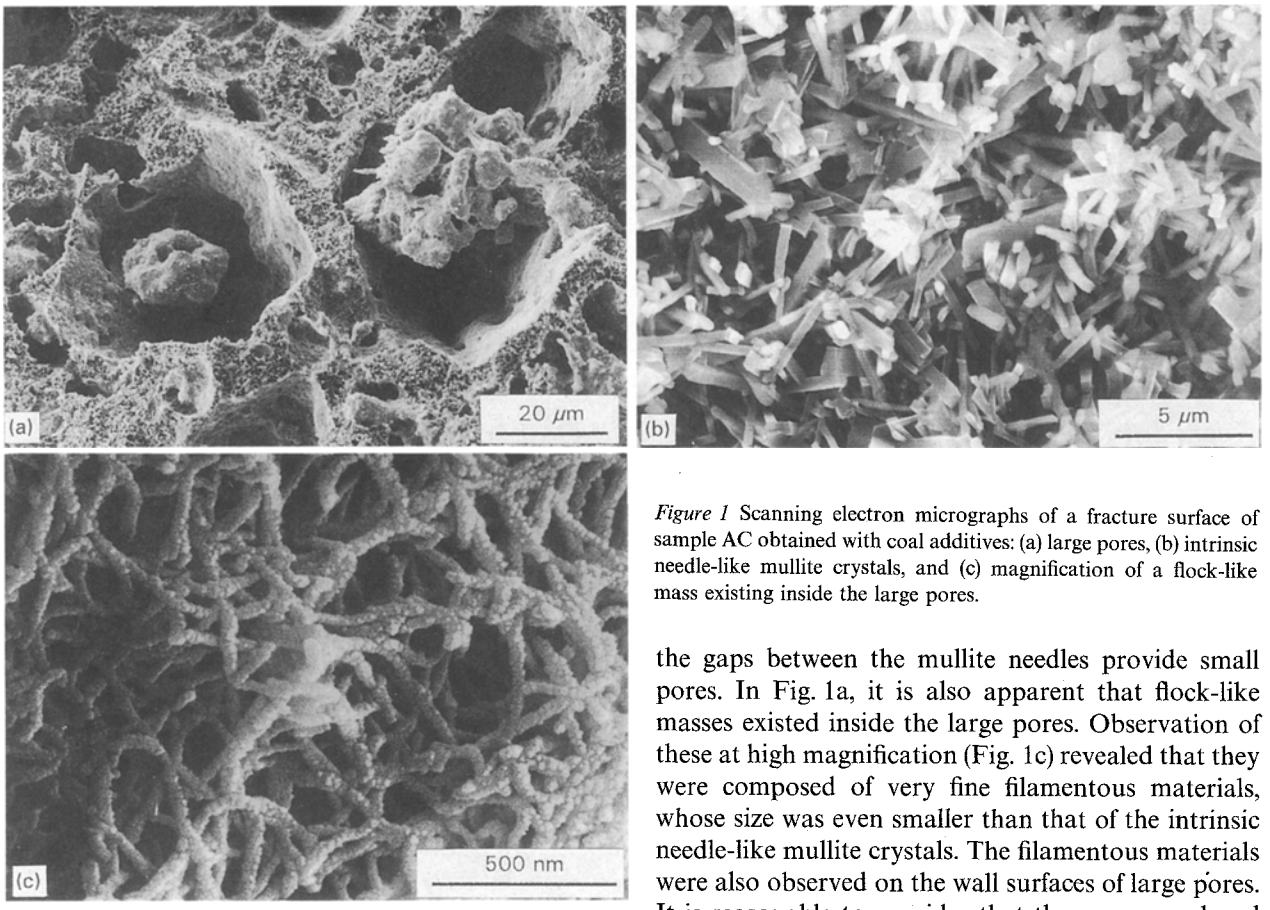

Figure 1 Scanning electron micrographs of a fracture surface of sample AC obtained with coal additives: (a) large pores, (b) intrinsic needle-like mullite crystals, and (c) magnification of a flock-like mass existing inside the large pores.

P denoting the kind of a pore former, coal and PMMA, respectively.

After adding a colloidal grade of cellulose (Asahi Kasei Co., RC 591) in 1 wt % to avoid segregation and separation, the suspensions were spread and dehydrated on a gypsum mould, followed by drying at 105 °C and firing at 1400 °C for 1 h. The heating rate was 100 °C h^{-1}. The calcined bodies were furnace cooled.

The calcined bodies were treated with a 5 mol l^{-1} sodium hydroxide solution in an autoclave at 150 °C under 5 atm to leach out the glass matrices [11]. Then the treated bodies were washed with an 1.0 mol l^{-1} hydrochloric acid solution, and were dried at 105 °C to obtain the final porous ceramics.

2.2. Characterization of porous ceramics

The crystallographic phases of the porous ceramics prepared were identified by the powder X-ray diffraction (XRD) method. Their microstructures were observed by scanning electron microscopy (SEM). A mercury porosimeter was employed to evaluate the size and distribution of pores.

3. Results and discussion

3.1. Pore structure with coal mixing

Fig. 1 shows scanning electron micrographs of a fracture surface of sample AC obtained with coal powder as a pore former. Large pores resulting from the coal particles were apparently observed at low magnification (Fig. 1a). The materials between large pores consisted of needle-like mullite crystals (Fig. 1b). Thus, the gaps between the mullite needles provide small pores. In Fig. 1a, it is also apparent that flock-like masses existed inside the large pores. Observation of these at high magnification (Fig. 1c) revealed that they were composed of very fine filamentous materials, whose size was even smaller than that of the intrinsic needle-like mullite crystals. The filamentous materials were also observed on the wall surfaces of large pores. It is reasonable to consider that they were produced from ash components of coal during firing and remained after leaching with a sodium hydroxide solution. XRD analysis of this sample, AC, indicated the presence of mullite as a main crystal phase and spinel $CoAl_2O_4$ as a minor phase. The spinel was also observed in sample A without coal addition [11]. On the other hand, it was found that the composition of coal ash was analogous to that of kaolin as a starting material, being composed mainly of SiO_2 and Al_2O_3. From these facts, it is more likely that the filamentous materials are very fine mullite crystals, though it is not conclusive.

The formation of the fine filamentous crystals should result in enlargement of the surface area. The BET surface area of sample AC was 31 $m^2 g^{-1}$, while it was 3.1 $m^2 g^{-1}$ for sample A without coal addition. In the case of sample BC, the formation of fine filamentous crystals was also observed, and the surface area increased from 12 $m^2 g^{-1}$ to 65 $m^2 g^{-1}$. Thus, the surface area of bimodal porous mullite ceramics prepared with the addition of coal powder became 5–10 times larger than that of the intrinsic porous ceramics due to the formation of very fine filamentous crystals. In the case of sample CC, however, fine filamentous crystals were not formed and there was no significant difference in surface area; 48 and 45 $m^2 g^{-1}$ for samples A and AC, respectively. The large surface area of sample C, compared with samples A and B, arises mainly from the considerably smaller size of the mullite needle crystals [11]. The reason why fine filamentous crystals were not formed in sample CC is not clear at present.

Fig. 2 shows pore-size distribution of the samples with and without coal additives. Sample AC showed

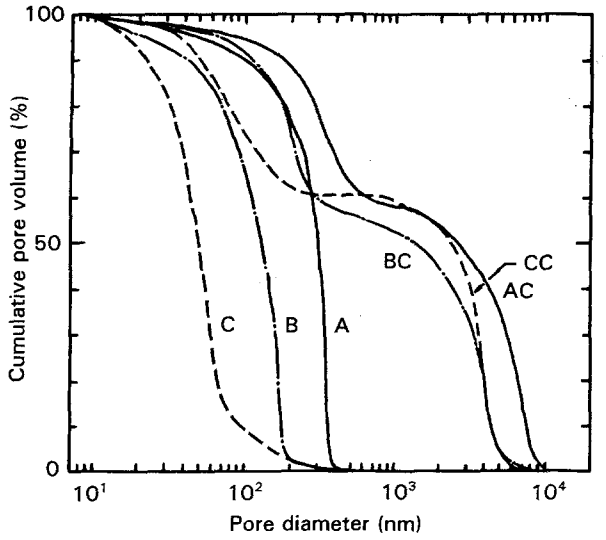

Figure 2 Pore-size distribution of porous mullite ceramics obtained with and without coal additives.

large pores with the median value of 5.8 μm in addition to small pores of 0.31 μm. Large and small pores are about 3.5 and 0.18 μm for sample BC, and 3.7 and 0.08 μm for sample CC, respectively. In all samples, the median values of the small pore size became larger than the intrinsic values of the samples without coal additives. This may be attributed to the enhanced crystal growth of mullite needles due to a small change in the SiO_2/Al_2O_3 composition by the coal ash and/or due to some catalytic effect of transition metal components in the ash. The size (3–6 μm) of large pores measured by a mercury porosimeter was much smaller than the particle size of the coal additives or the pore size measured by SEM observation in every case. Therefore, it is considered that the value of 3–6 μm corresponds to the entrance diameter at the neck part of the neighbouring large pores. Namely, it may be considered that the large pores are ink-bottle type in shape.

Assuming that the size and shape of the coal particles employed were inherited in the large pores after firing and that their shrinkage during calcining was the same as that of the green materials, kaolin plus transition metal oxides, the volume percentage of total pores, P, and that of large pores, P_L, can be related to the weight per cent of pore-forming materials, W, as follows

$$P = \frac{[(100 - W)k/D_b + W/D_p] \times 100}{(100 - W)/D_b + W/D_p)} \quad (1)$$

$$P_L = \frac{(W/D_p) \times 100}{(100 - W)/D_b + W/D_p} \quad (2)$$

where D_b is the bulk density of the green materials on the dry base, D_p the density of a pore former, and k the porosity of intrinsic porous ceramics when no pore former is used. D_b was 1.31 g cm^{-3} for all samples, and D_p was 1.38 g cm^{-3} for coal. The measured k values were 0.55, 0.54 and 0.58 for samples A, B and C, respectively.

Table I compares the calculated pore volumes with the experimental data determined by mercury porosimetry. The observed total pore volume was in the range 72–76 vol %. The values were smaller only by approximately 2 vol % than the calculated ones in the cases of samples AC and BC, whereas the experimental and calculated values were almost comparable to each other in sample CC. For the large pore volume, values of 56–60 vol % were observed and again agreed well with the calculated values, with a maximum deviation of 3 vol %. Thus, it is obvious that the volume percentages of total and large pores can be estimated using Equations 1 and 2, respectively, in the case of the present bimodal porous ceramics.

TABLE I Volume percentage of total and large pores in the bimodal porous ceramics obtained with coal additives

Sample	Total pore volume, P(%)		Large pore volume, P_L(%)	
	Observed	Calculated	Observed	Calculated
AC	72.1	74.6	58.0	58.5
BC	71.8	74.1	56.0	59.0
CC	76.0	76.4	60.0	57.2

3.2. Pore structure with PMMA mixing

As described above, very fine filamentous crystals were formed in the space of large pores when coal was employed as a pore-forming material, in addition to the intrinsic needle-like mullite crystals. This finding is of interest in a sense that enlargement of specific surface area is possible and the resultant porous ceramics may be useful as a good catalyst support. However, the resultant pore structure is not strictly bimodal but trimodal, although the trimodal feature was not clear in the curves of pore-size distribution, because of a very small volume fraction of the smallest pores. The existence of such very small pores may present some problems in other applications mentioned in Section 1. This prompted us to examine the usefulness of PMMA beads, which do not leave any ash, as a pore-forming material.

Fig. 3 shows scanning electron micrographs of a fracture surface of sample AP obtained with PMMA additives. In Fig. 3a, it is seen that large pores resulting from spherical PMMA beads are densely distributed in the sample. Thus, the shape and size of the beads were inherited in the large pores after firing and leaching. On the other hand, the thickness of the walls between large pores was of the order of several micrometres (Fig. 3b). Fig. 3b also indicates the presence of some pathways (the dark part in the photograph) from one pore to neighbouring pores. The shape of the pathways was irregular, but their size was roughly of the order of several micrometres. It may be possible to control the size of the pathways by changing the amount of the beads; an increase in the amount would result in enlargement of the pathways. The morphology of the crystals was only observed to be intrinsic mullite needles, and the fine filamentous crystals, which were formed in the samples with coal additives, were not observed in this case of PMMA additives.

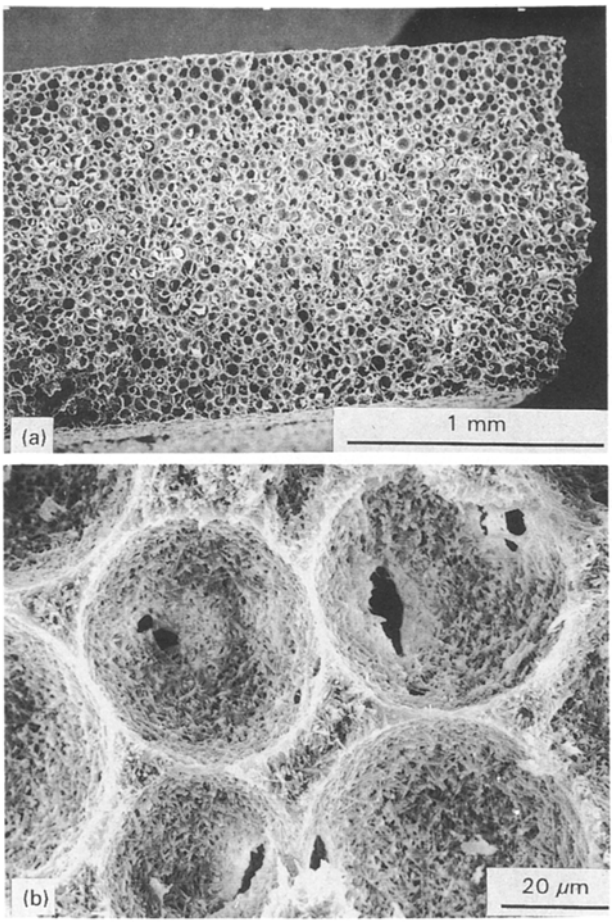

Figure 3 Scanning electron micrographs of a fracture surface of sample AP obtained with PMMA additives.

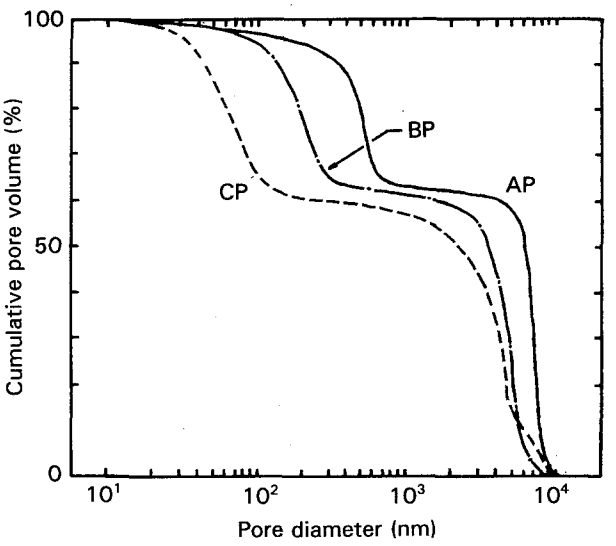

Figure 4 Pore-size distribution of porous mullite ceramics obtained with the PMMA additives.

TABLE II Volume percentage of total and large pores in the bimodal porous ceramics obtained with PMMA additives

Sample	Total pore volume, P(%)		Large pore volume, P_L(%)	
	Observed	Calculated	Observed	Calculated
AP	75.6	76.5	63.0	62.4
BP	75.1	76.0	62.0	62.9
CP	75.3	78.1	61.0	61.2

Fig. 4 shows pore-size distribution of three samples obtained with the addition of 45 wt % PMMA. Bimodal pore characteristics are apparent from individual curves. The curves in the large pore region are steeper than those in Fig. 2, indicating the sharper pore distribution than in the samples of coal addition. However, the median values of pore size of 4–8 μm, which were determined by mercury porosimetry, were smaller by approximately an order of magnitude, than the SEM pore diameter or that of PMMA beads. Thus, it is reasonable to consider that the size of large pores observed in Fig. 4 corresponds to that of the open pathways between the large pores, as in the case of the samples with coal additives.

On the other hand, the median value of small pores in sample AP was 0.49 μm, which was slightly larger than that of sample AC. This apparent increase in size of small pores may be attributed to the lack of formation of very fine filamentous crystals in the case of PMMA addition. Small pores in sample BP showed a median value of 0.18 μm, which was the same as that in sample BC. In the case of sample CP, the median value was 0.06 μm, being smaller than that of sample CC. These variations arise probably from different rates of crystal growth of mullite needles. However, the details are not clear at present.

The volume percentages of total and large pores in the samples with PMMA additives were calculated, again using Equations 1 and 2, respectively. The density of PMMA beads, $D_p = 1.17\ g\,cm^{-3}$, was used in the calculation, and the results are given in Table II. Observed total pore volume values of 75–76 vol % again agreed well with the calculated values within a deviation of 1–3 vol %. In addition, the observed value of the percentage of large pore volume could be well expressed by Equation 2 within a small error.

4. Conclusion

Bimodal characteristics of pore-size distribution could be realized by mixing coal powder or PMMA beads as a pore-forming material into the starting material of mullite ceramics, followed by firing and leaching of the glass matrices surrounding the needle-like crystals. The shape and size of the pore formers were inherited by the large pores formed. This presents the possibility that the size of large pores may be controlled by employing pore-forming materials with different sizes. The smaller pores, of size 0.05–0.5 μm, in the bimodal porous ceramics corresponded to the space between the needle-like mullite crystals. On the other hand, the median size of larger pores resulting from pore formers was determined to be 3–7 μm by mercury porosimetry. The values were much smaller than the pore size observed by SEM, implying that the pores are ink-bottle type in shape. The observed volume percentages of total and large pores in the samples coincided well with the calculation based on the bulk density of raw materials, the amount of pore formers, and the intrinsic porosity of the mullite ceramics. In the case of the coal addition, very fine filamentous crystals were formed, probably due to the effect of the

ash components, in addition to the intrinsic needle-like mullite crystals. As a result, the surface area of the porous ceramics became larger by a factor of 5–10, than the intrinsic ceramics, the largest value being 65 $m^2 g^{-1}$.

References

1. N. HARA and H. TAKAHASHI, "Zeolite" (Kohdansha, Tokyo, 1980) p. 89.
2. H. YANAI, "Kyuchaku Kogaku Yoran", (Kyoritsu Shuppan, Tokyo, 1977) p. 101.
3. Y. KATOH, *Taikabutsu* **40**(3) (1988) 42.
4. H. HORITSU, Y. MASEDA and K. KAWAI, *Agric. Biol. Chem.* **54**(2) (1990) 295.
5. K. NAKANISHI, H. MURAYAMA, K. SATO, H. NAGAE, T. YASUI and S. MITSUI, *Hakkoh Kogaku Kaishi* **67** (1989) 509.
6. C. GHOMMIDH, J. M. NAVARRO and G. DURANDO, *Biotech. Bioeng.* **24** (1982) 605.
7. Y. SHIMIZU, M. ROKUDAI, Y. TOHYA, E. KAYAWAKE, T. YAZAWA, H. TANAKA and K. EGUCHI, *Kagaku Kogaku Ronbunshu* **14** (1988) 818.
8. S. TAKADA and S. WAKABAYASHI, *Zohsui Gijutsu* **12**(4) (1986) 49.
9. T. OKUYAMA, *Bull. Ceram. Soc. Jpn* **24** (1989) 633.
10. H. ABE, H. SEKI, A. FUKUNAGA and M. EGASHIRA, *J. Ceram. Soc. Jpn* **97** (1989) 604.
11. H. ABE, H. SEKI, A. FUKUNAGA, H. TSUZUKI and M. EGASHIRA, *ibid.* **98** (1990) 339.
12. H. ABE, H. SEKI, A. FUKUNAGA and M. EGASHIRA, *ibid.* **100** (1992) 33.

Received 3 August 1992
and accepted 31 August 1993